

Time-dependent CP violation results at Belle II

M. Veronesi, on behalf of the Belle II Collaboration

Iowa State University, Ames, USA

We report updates on time-dependent CP -violation observables at Belle II. The benchmark measurements of the B^0 lifetime τ_{B^0} and mixing frequency Δm_d using flavor specific hadronic decays and the determination of the CP -violating phase $\sin 2\phi_1$ in $b \rightarrow c\bar{c}s$ transitions have been performed using data collected between 2019–2021. These analyses use only half of the current available dataset and are still statistically limited, showing the excellent performance of the detector and readiness of the analysis tools. We present three new results on the effective value of $\sin 2\phi_1$ in $b \rightarrow q\bar{q}s$ transitions, which are highly sensitive to generic non-Standard Model (SM) physics amplitudes, using the full dataset collected between 2019–2022.

1 Introduction

Measurements of the B^0 mixing frequency Δm_d with flavor-specific decays and the determination of the CP -violating phase $\sin 2\phi_1$ in $b \rightarrow c\bar{c}s$ transitions are important elements to constrain the unitarity of the Cabibbo-Kobayashi-Maskawa (CKM) matrix in the SM. On the other hand, measurements of time-dependent CP -violation in $b \rightarrow q\bar{q}s$ transitions offer a powerful probe for generic new physics, as they proceed through loop-suppressed decays which are potentially affected by non-SM amplitudes¹. However, this class of decays usually involves neutral particles in the final state, that are experimentally challenging to reconstruct. This, combined with the small branching fractions, makes the current average of available measurements statistically less precise than the theory prediction. Belle II is in the unique position to improve the current experimental knowledge due to its capabilities with vertex determination and efficient reconstruction of neutral particles.

Belle II² is a high-energy physics experiment at the SuperKEKB collider³, operating at the $\Upsilon(4S)$ resonance. The detector is designed to reconstruct the decays of heavy mesons and τ leptons in energy-asymmetric e^+e^- collisions. Of particular importance for the measurement of time-dependent observables is the innermost part of the detector, equipped with a two-layer silicon pixel detector (PXD), surrounded by a four-layer double-sided silicon-strip detector (SVD). The dataset used for the analyses presented here was collected with only one sixth of the second PXD layer installed. $B\bar{B}$ events are produced in a quantum-entangled state from the decay of an $\Upsilon(4S)$ resonance. The proper-time difference Δt is estimated using the decay vertex positions of the two B mesons in the event along the boost axis. In spite of the lower boost compared to KEKB, the upgraded detector is able to achieve a better vertex resolution than its predecessor. In addition, the knowledge of decay times is enhanced by the constraint from the beam spot profile in combination with the new nano-beam scheme, achieving a Δt resolution of less than 1 ps.

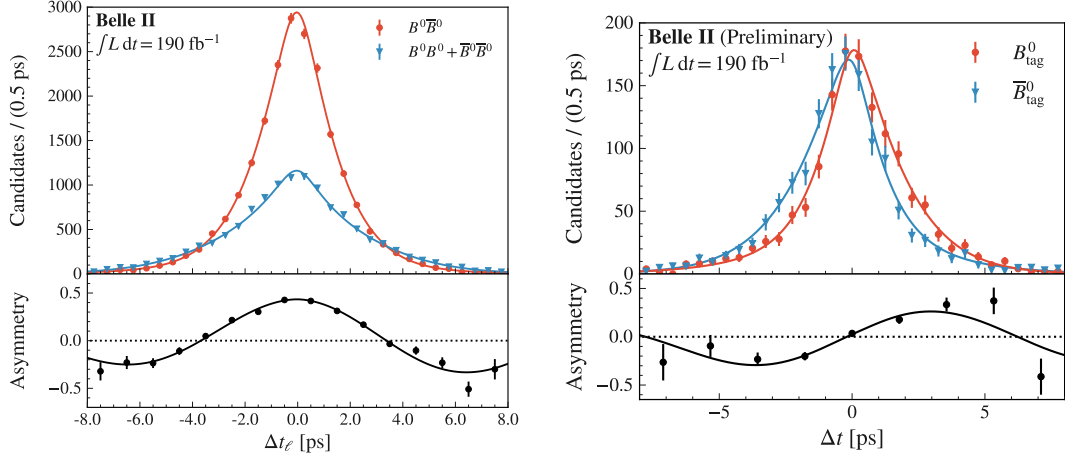


Figure 1 – Projections of the Δt fit on the $B^0 \rightarrow D^{(*)-}\pi^+$ (left) and $B^0 \rightarrow J/\psi K_S^0$ (right) samples.

2 Measurement of τ_{B^0} , Δm_d and $\sin 2\phi_1$ with 2019–2021 data

The distribution of the decay time difference Δt for flavor-specific B^0 decays is:

$$\mathcal{P}(\Delta t, q) = \frac{e^{-|\Delta t|/\tau_{B^0}}}{4\tau_{B^0}} \left\{ 1 + q \cos(\Delta m_d \Delta t) \right\}, \quad (1)$$

where τ_{B^0} is the B^0 lifetime, Δm_d is the $B^0 - \bar{B}^0$ mixing frequency, and q is $+1$ (-1) when the two B mesons have the opposite (same) flavor. The flavor of the other B^0 is identified using a category-based B -flavor tagging algorithm⁴ from the inclusive properties of particles in the event that are not associated with the signal candidate.

The measurement of τ_{B^0} and Δm_d allows to test the QCD theory of strong interactions at low energy⁵ and to constrain the side of the CKM triangle. In addition, one is able to experimentally determine the Δt resolution function and flavor tagging parameters diluting the observable oscillations. These inputs are needed for the measurement of time-dependent CP asymmetries in B^0 decays to CP eigenstates, for which the Δt distribution is:

$$\mathcal{P}(\Delta t, q) = \frac{e^{-|\Delta t|/\tau_{B^0}}}{4\tau_{B^0}} \left\{ 1 + q [A \cos(\Delta m_d \Delta t) + S \sin(\Delta m_d \Delta t)] \right\}, \quad (2)$$

where q is the flavor of the other B^0 in the event ($q = +1$ for B^0 and $q = -1$ for \bar{B}^0), and A and S are the direct and mixing induced CP asymmetries. For $B^0 \rightarrow J/\psi K_S^0$ decays, the values of A and S are expected to be equal to zero and $\sin 2\phi_1$, respectively, in the SM.

The most recent Belle II analyses^{6,7} are based on a sample of 190 fb^{-1} collected at the $\Upsilon(4S)$ center-of-mass energy and corresponding to 200×10^6 $B\bar{B}$ pairs. We reconstruct 33317 signal $B^0 \rightarrow D^{(*)-}\pi^+$ decays and 2755 signal $B^0 \rightarrow J/\psi K_S^0$ events. The background-subtracted⁸ Δt distributions and corresponding flavor specific and mixing induced CP asymmetries are shown in Fig. 1. The measured lifetime, mixing frequency and CP asymmetries are reported in Tab. 1 together with the world average values⁹. For the lifetime and mixing measurements, the largest sources of systematic uncertainty are due to the resolution function parameters fixed from simulation and detector misalignment. For the determination of the direct and mixing-induced CP asymmetries, the dominant sources of systematic uncertainty are the tag-side interference (*i.e.* the presence of $b \rightarrow u\bar{c}d$ Cabibbo-suppressed decay in the tagging B^0) and the limited statistical knowledge of the flavor tagging and resolution parameters from the $B^0 \rightarrow D^{(*)-}\pi^+$ calibration sample. Although not yet as precise as the current world-leading measurements, these results are still statistically limited and have systematic uncertainties comparable to those of previous generation B -factories.

Table 1: Comparison of recent Belle II results (where the first uncertainties are statistical, while the second are systematic) and world average values of the B^0 lifetime, mixing frequency and CP asymmetries in $b \rightarrow c\bar{c}s$ transitions.

Observable	Belle II (190 fb $^{-1}$)	World Average
τ_{B^0}	$1.499 \pm 0.013 \pm 0.008$ ps	1.519 ± 0.004 ps
Δm_d	$0.516 \pm 0.008 \pm 0.005$ ps $^{-1}$	0.5065 ± 0.0019 ps $^{-1}$
$A(b \rightarrow c\bar{c}s)$	$0.094 \pm 0.044^{+0.042}_{-0.017}$	0.005 ± 0.015
$S(b \rightarrow c\bar{c}s)$	$0.720 \pm 0.062 \pm 0.016$	0.699 ± 0.017

3 Measurement of $\sin 2\phi_1$ in $b \rightarrow q\bar{q}s$ transitions with 2019-2022 data

The decays $B^0 \rightarrow \phi K_S^0$, $B^0 \rightarrow K_S^0 K_S^0 K_S^0$ and $B^0 \rightarrow K_S^0 \pi^0$ all proceed through $b \rightarrow q\bar{q}s$ gluonic penguin transitions and therefore provide inputs to the effective value of $\sin 2\phi_1$. Belle II has recently reported three new measurements using a sample of 362 fb $^{-1}$, corresponding to 387×10^6 $B\bar{B}$ pairs. The three analyses adopt similar techniques to separate signal from background, *e.g.* multi-dimensional likelihood fits the beam-constrained mass M_{bc} , energy difference ΔE and transformed output of the classifier \mathcal{O}'_{CS} combining several continuum suppression variables. In addition, they use the flavor tagging and, in the case of $B^0 \rightarrow \phi K_S^0$, resolution function parameters from the $B^0 \rightarrow D^{(*)-} \pi^+$ calibration sample. The background-subtracted⁸ Δt distributions are displayed in Fig. 2 and the measured CP asymmetries are reported in Tab. 2.

3.1 $B^0 \rightarrow \phi K_S^0$

The $B^0 \rightarrow \phi K_S^0$ decay vertex is reconstructed from the two prompt tracks of the $\phi \rightarrow K^+ K^-$ decay, therefore, it has a similar Δt resolution as the $B^0 \rightarrow J/\psi K_S^0$ mode. In addition to the dominant continuum $q\bar{q}$ background, it suffers from a sizeable contribution from non-resonant $B^0 \rightarrow K^+ K^- K_S^0$ decays with the same final state but opposite CP eigenvalue, diluting the observable CP asymmetries. In order to disentangle the non-resonant background component, we perform a multidimensional fit including the cosine of the helicity angle, in which the $B^0 \rightarrow \phi K_S^0$ and $B^0 \rightarrow K^+ K^- K_S^0$ have different distributions. In total, we reconstruct 162 ± 17 signal $B^0 \rightarrow \phi K_S^0$ and 21 ± 12 background $B^0 \rightarrow K^+ K^- K_S^0$ events. We estimate the residual effect of neglecting interference using a MC sample generated with a complete Dalitz description of the decay. The analysis is validated on generic MC and on the $B^+ \rightarrow \phi K^+$ control channel in data, which features similar backgrounds, vertexing and null CP asymmetries. The statistical sensitivity on A is on par with the world's best measurements. When compared to the Belle¹⁰ and BABAR¹¹ analyses using a similar quasi-two body strategy, there is a 10 to 20% statistical improvement on S for the same number of signal events. The dominant sources of systematic uncertainty stem from the bias induced by the fit model used to disentangle signal from backgrounds and neglecting the contribution from additional mis-reconstructed $B\bar{B}$ backgrounds in the fit.

3.2 $B^0 \rightarrow K_S^0 K_S^0 K_S^0$

The $B^0 \rightarrow K_S^0 K_S^0 K_S^0$ decay proceeds through the same underlying $b \rightarrow s\bar{s}s$ quark transition as of $B^0 \rightarrow \phi K_S^0$. It has the advantage of not being affected from opposite- CP backgrounds. However, since K_S^0 decay on average outside of the pixel detector, it is experimentally challenging due to the absence of prompt tracks to form a vertex. The decay vertex reconstruction relies on the K_S^0 trajectory and profile of the interaction point. In order to achieve the best statistical sensitivity, the dataset is divided into “time-differential” (TD) events, for which the K_S^0 carry sufficient information from the vertex detector, and “time-integrated” (TI) events, for which the decay vertex is poorly constrained. The TD events are used in the time-dependent CP fit, while TI events are used only to measure A . In addition, the resolution function parameters obtained in

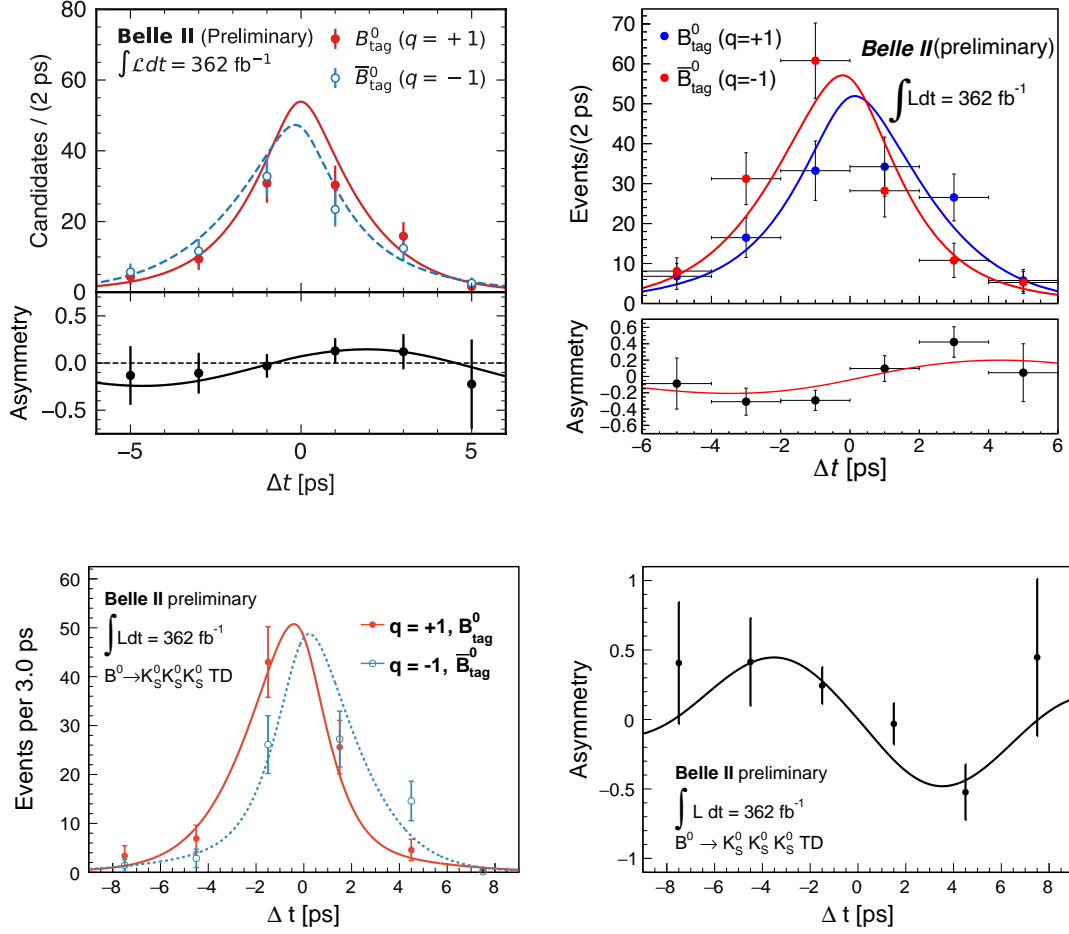


Figure 2 – Projections of the Δt fit and CP asymmetries in $b \rightarrow q\bar{q}s$ decays: $B^0 \rightarrow \phi K_S^0$ (top left), $B^0 \rightarrow K_S^0\pi^0$ (top right) and $B^0 \rightarrow K_S^0 K_S^0 K_S^0$ (bottom).

simulation are scaled in data by including the $B^+ \rightarrow K_S^0 K_S^0 K^+$ control channel in the combined fit. In total, we reconstruct 158_{-13}^{+14} TD and 62 ± 9 TI events. The statistical sensitivity on A is on par with the world's best measurements. The leading sources of systematic uncertainty are the bias induced by the fit model and calibration of the flavor tagging.

3.3 $B^0 \rightarrow K_S^0\pi^0$

The $B^0 \rightarrow K_S^0\pi^0$ decay belongs to the same class of $b \rightarrow q\bar{q}s$ decays as $B^0 \rightarrow \phi K_S^0$ and $B^0 \rightarrow K_S^0 K_S^0 K_S^0$. It has a higher effective branching fraction than $B^0 \rightarrow \phi K_S^0$ and $B^0 \rightarrow K_S^0 K_S^0 K_S^0$ but slightly larger theoretical uncertainties¹. The signal reconstruction requires excellent performance with neutrals, due to the absence of prompt tracks and presence of a π^0 in the final state. The analysis follows a similar strategy as $B^0 \rightarrow K_S^0 K_S^0 K_S^0$, dividing the dataset into TD and TI events to retain the information on A from events with poor Δt resolution. In total, we reconstruct 415_{-25}^{+26} signal events. The analysis strategy is validated on $B^0 \rightarrow J/\psi K_S^0$ data, reconstructed without the vertex information from the J/ψ . The statistical sensitivity on A and S is already on par with the world's best determinations in spite of the smaller dataset. The dominant contribution to the systematic uncertainty arise from neglecting possible CP asymmetries in the backgrounds and from the calibration of the resolution function.

Table 2: Comparison of recent Belle II results (where the first uncertainties are statistical, while the second are systematic) and world average of CP asymmetries in $b \rightarrow q\bar{q}s$ transitions.

Observable		Belle II (362 fb ⁻¹)	World Average
$B^0 \rightarrow \phi K_S^0$	A	$0.31 \pm 0.20^{+0.05}_{-0.06}$	-0.01 ± 0.14
	S	$0.54 \pm 0.26^{+0.06}_{-0.08}$	$0.74^{+0.11}_{-0.13}$
$B^0 \rightarrow K_S^0 K_S^0 K_S^0$	A	$0.07^{+0.15}_{-0.20} \pm 0.02$	0.15 ± 0.12
	S	$-1.37^{+0.35}_{-0.45} \pm 0.03$	-0.83 ± 0.17
$B^0 \rightarrow K_S^0 \pi^0$	A	$0.04^{+0.15}_{-0.14} \pm 0.05$	-0.01 ± 0.10
	S	$0.75^{+0.20}_{-0.23} \pm 0.04$	0.57 ± 0.17

4 Summary

Belle II has performed measurements of the B^0 lifetime and mixing frequency with flavor-specific decays and CP asymmetries in $b \rightarrow c\bar{c}s$ transitions using half of its dataset. These high-yield analyses require the accurate modeling of the vertex resolution and flavor tagging response, which represent important milestones in the development of time-dependent analyses. In addition, we report recent results on CP violation in $b \rightarrow q\bar{q}s$ transitions using the full Belle II datasets, where some observables are already competitive with the world's most precise measurements, albeit using much less luminosity. Due to its excellent neutral reconstruction capabilities, Belle II is in the unique position to improve our current experimental knowledge on these modes, that are essential to probe generic non-SM physics in loops.

References

1. M. Beneke. Corrections to $\sin(2\beta)$ from CP asymmetries in $B^0 \rightarrow (\pi^0, \rho^0, \eta, \eta', \omega, \phi)K_S^0$ decays. *Phys. Lett. B*, 620:143–150, 2005.
2. T. Abe. Belle II Technical Design Report. 2010.
3. Kazunori Akai, Kazuro Furukawa, and Haruyo Koiso. SuperKEKB collider. *Nucl. Instrum. Meth.*, A907:188, 2018.
4. F. Abudinén et al. B-flavor tagging at Belle II. *Eur. Phys. J. C*, 82(4):283, 2022.
5. Alexander Lenz. Lifetimes and heavy quark expansion. *Int. J. Mod. Phys. A*, 30(10):1543005, 2015.
6. I. Adachi et al. Measurement of decay-time-dependent CP violation in $B^0 \rightarrow J/\psi K_S^0$ decays using 2019-2021 Belle II data. 2 2023.
7. F. Abudinén et al. Measurement of the B^0 lifetime and flavor-oscillation frequency using hadronic decays reconstructed in 2019-2021 Belle II data. 2 2023.
8. Muriel Pivk and Francois R. Le Diberder. sPlot: A statistical tool to unfold data distributions. *Nucl. Instrum. Meth.*, A555:356–369, 2005.
9. Yasmine Sara Amhis et al. Averages of b-hadron, c-hadron, and τ -lepton properties as of 2021. *Phys. Rev. D*, 107(5):052008, 2023.
10. K.-F. Chen et al. Observation of Time-Dependent CP Violation in $B^0 \rightarrow \eta' K^0$ Decays and Improved Measurements of CP Asymmetries in $B^0 \rightarrow \phi K^0$, $K_S^0 K_S^0 K_S^0$ and $B^0 \rightarrow J/\psi K^0$ Decays.
11. Bernard Aubert et al. Measurement of CP asymmetries in $B^0 \rightarrow \phi K^0$ and $B^0 \rightarrow K^+ K^- K_S^0$ decays. *Phys. Rev. D*, 71:091102, 2005.